

SYNTHESIS AND CHARACTERIZATION OF MgB_2 SUPERCONDUCTORS WITH CARBON NANOTUBES (CNTs) AND TIN (Sn) ADDITION

Hendrik✉

*Research Center for Advanced Materials¹
hend028@brin.go.id*

Muhammad Nur Farhanudin
Department of Physics²

Nono Darsono
Research Center for Advanced Materials¹

Satrio Herbirowo
Research Center for Advanced Materials¹

Darminto
Department of Physics²

Andika Widya Pramono
*Research Center for Advanced Materials¹
Faculty of Technology and Energy Business³*

Agung Imaduddin
Research Center for Advanced Materials¹

¹*National Research and Innovation Agency
PUSPIPTEK, Tangerang Selatan, Banten, Indonesia, 15314*

²*Institut Teknologi Sepuluh Nopember
Kampus ITS Sukolilo – Surabaya, Jawa Timur Indonesia, 60111*

³*Institute of Technology PLN – Menara PLN, Jalan Lingkar Luar Barat,
Duri Kosambi – Jakarta Barat Indonesia 11750*

✉ **Corresponding author**

Abstract

MgB_2 /CNT is a promising candidate for superconducting wire application due to its excellent mechanical properties and carbon nanotube's low density. However, strong interfacial adhesion between the CNT reinforcement and the MgB_2 matrix is difficult to manage. Therefore, this study examines the synthesis and characterization of magnesium diboride (MgB_2) superconductors with carbon nanotubes (CNTs) and tin (Sn) addition. Determining the proper method and combination of CNT & Sn affects MgB_2 superconductors is crucial. Raw materials of magnesium (Mg), boron (B), Sn, and multi-walled carbon nanotubes (MWCNTs) were used for a solid-state reaction process to determine the proper synthesis method and the effect of CNT on superconductors' critical temperature. Each sample was obtained by weighing the raw material first, followed by hand grinding with agate mortars for 3 hours. The pelletization was then conducted by using a compact pressing machine with a pressure of 350 MPa. The compacted samples were then sintered at 800 °C for 2 hours either through the vacuum or PIST process. Finally, all were characterized, and MgB_2 was discovered to be the dominant phase with minor impurity phases such as MgO, Mg, Mg_2Sn , C, and Sn. Based on SEM morphological analysis, the grain boundaries of sample A1 were more precise than B2. In both, the grain size also varies, and the distribution of elements is uneven. Subsequently, Cryogenic Magnet Characterization indicated that at 40 K, almost all samples possess superconducting characteristics. For future studies, the potential impact of MgB_2 on critical current density (J_c) and magnetic density (H_c) in several commercial applications such as Magnetic Resonance Imaging (MRI), magnetic levitation, and transformers needs to be investigated.

Keywords: MgB_2 , CNT, wire, morphological, solid-state reaction, cryogenic, MRI, sintered, SEM, XRD.

DOI: 10.21303/2461-4262.2022.002419

1. Introduction

Due to the low cost and wide availability of raw materials, MgB_2 , a binary intermetallic compound, is one of the most promising superconductors for electrical applications, namely sensor [1], energy storage [2], and wire [3]. Hence, MgB_2 and its systems, as well as superconductivity, have been continually developed because of its functional properties such as high T_c of 39 K, weak-link free grains, lightweight, and increased coherence [4, 5]. Moreover, the high critical current density (J_c) at high fields and temperatures is the primary concern for magnesium diboride to substitute low-temperature superconductors. For example, increasing pressure has a significant superconducting correlation with composite MgB_2 [6]. In most applications, MgB_2 needs to meet some requirements, including high thermal stability, excellent mechanical stability, and inert behavior [7]. The number of MgB_2 wire filaments is significant during wire processing [8]. This prompts scientists to enhance the compound's performance because of the sensitivity of critical current density to increase its magnetic fields [9].

Several methods have been used to synthesize MgB_2 superconductors, such as direct microwave synthesis [10], high-energy ball milling [11], infiltration, and growth process [12]. Chemical modification such as doping is still the most attractive and effective way to improve the properties of magnesium diboride [13, 14]. CNT dopants [15] discovered that the connectivity of undoped ex-situ MgB_2 often decreases.

Substitutional doping is a significant means of enhancing superconductivity. Once MgB_2 is doped with carbon contents, these mixtures have an enormous potential to impact the superconducting mechanism and the distributed electron, thereby reducing the free path & coherence length. The nano-order carbon (CNT) doping effect has a coherence length comparable to MgB_2 [16]. CNT that is successfully doped with (boron) B increases the critical electrical current density (J_c) of MgB_2 by using an external magnetic field. However, the amorphous C-doped sample decreases the J_c performance [17]. In the selected powder-in-sealed-tube (PIST) method, Mg and B powder were used as raw materials because of their excellent influence on MgB_2 microstructure and superconducting properties. A previous study has reported the production of MgB_2 monofilament wire through the PIST [18]. However, oxides presence and the usage of argon gas which tends to be expensive, is still the main problem faced; therefore a cheaper method that produces good results is employed.

This study aimed to improve the phase transformation, normal-state conductivity, and mechanical strength of MgB_2 for more acceptability in wire manufacture [19], as well as to analyze the effect of vacuum and powder-in-sealed-tube synthesis methods, which was confirmed by the characteristics of impurities formed, microstructure, and low temperature zero resistance. Besides, the effect of Sn and CNT elements addition on the superconductivity of MgB_2 was determined.

2. Materials and methods

2. 1. Materials preparation

Using stoichiometric mixtures of commercial Mg powder and amorphous B powder as precursors, all MgB_2 PIST samples were prepared through the in-situ route. According to **Table 1**, all the starting materials, namely magnesium powder, boron, multi-walled carbon nanotubes, and tin.

Table 1

The weight ratio of materials

Sample	wt (gr)		
	Mg	B	Sn
A1	0.51842	0.46158	0.01
A2	0.51313	0.45687	0.01
A3	0.49726	0.44274	0.01
B1	0.51842	0.46158	0.01
B2	0.51313	0.45687	0.01
B3	0.49726	0.44274	0.01

2. 2. Synthesis of MgB₂ bulk vacuum method

Magnesium (Mg) powder, boron (B), tin (Sn), and multi-walled carbon nanotubes (MWCNTs) were weighed using a digital balance according to their stoichiometric calculations. Three kinds of samples with different mass composition materials were obtained from the preparation and measurement process. Then, each was crushed by hand (hand milling) for 3 hours in a container called agate mortar to make the sample constituents homogeneous.

The crushed samples were printed into pellet form using BMI Simon Machinery MFG.CO compacting machine with a pressure of 350 MPa. The sample's powder was put into the machine's dies and placed very parallel to the pressure lever. After switching on the power button, the drive lever was moved until the dies were pressed and held for a while. When the driving lever was lifted, and the dies were removed, the initial powder had become a more solid-shaped pellet prepared for the sintering process.

2. 3. Synthesis of MgB₂ bulk Powder-in-Sealed-Tube (PIST) Method

In the synthesis of samples with PIST, the principle was the same as that of the vacuum. The difference was that the media used to obtain the vacuum condition in this method was a tube made of stainless steel, namely SS 316. To avoid oxidation in the constituent elements, SS 316 tubes were prepared first by cutting 8 cm in length with a 12 cm diameter, followed by trimming the edges from the former piece. The SS 316 was then placed in a container and soaked with a nitric acid solution for one day to obtain a sterile result or prevent contamination from other ingredients in the tubes. Subsequently, the SS 316 tubes were washed with plain water and dried. After being scorched, the tube was compacted at one end by a compacting machine until it became tight or stopped allowing air to come in and out.

Furthermore, sample preparation was performed using magnesium powder, boron powder, and carbon nanotubes (CNTs) with a 1; 2; 5 wt. %, respectively. Each variation's calculations and mass values were the same as those used previously (**Table 1**). PIST method samples were also prepared to support this study by adding only tin (Sn) and MgB₂ without other ingredients. After compacting all samples, the following process was sintering, where the principle was the same as in the vacuum method, but the furnace employed was a type that does not use cylinders and pumping machines. The samples were heated in the furnace for 2 hours with a target temperature of 800 °C. The target temperature is obtained 3 hours from turning on the furnace machine in the implementation.

2. 4. Material characterization

The synthesized samples were characterized by x-ray diffraction (XRD) (Bruker AXS θ -2 θ) with Cu K- α radiation of 1.5406 Å, operated at 40 kV and 40 mA with advanced analysis of the database International Centre for Diffraction Data (ICDD) PDF-2 No. 96-100-0027. The morphology of the formed microstructure was confirmed by observing using scanning electron microscopy (SEM) (JEOL6390A). Cryogenic Magnet measured the superconducting properties by Cryotron Oxford Instrument 5 K.

3. Results and Discussion

The results of the XRD pattern on the MgB₂ sample (vacuum and PIST method) showed that there was only one the highest diffraction peak located at 2θ of 42.470° according to *International Centre for Diffraction Data (ICDD) PDF-2 No. 96-100-0027*, this indicated that the synthesis result of magnesium boron in the form of Mg+B could convert into MgB₂ phase.

The result of XRD testing in **Fig. 1**, the formed MgB₂ phase, which can be observed from the peaks of the diffraction pattern at angles of 33.5226°, 42.4292°, 51.7959°, 59.9325° & 63.3049° for sample code A1, 33.5879°, 42.4743°, 51.8190°, 59.9844°, 63.1796° & 66.3850° for A2, and 33.5903°, 34.3138°, 42.4350°, 51.7989°, 60.0547°, 63.1932° & 66.2117° for A3. This is by the International Center for Diffraction Data (ICDD) PDF-2 No. 96-100-0027. Besides the MgB₂, minor phases (impurities) such as MgO, C, & Sn are detected when analyzed and further processed to determine each fraction. Nevertheless, the peaks of the MgB₂ phase obtained have a high intensity and are mainly

formed compared to the impurities; hence, in sample code A, the MgB_2 is the dominant phase. Based on the XRD result, the MWCT dopant causes ratio (c/a) change in the crystal structure of samples A1, A2, & A3 to 1.145, 1.145, & 1.147, respectively [20].

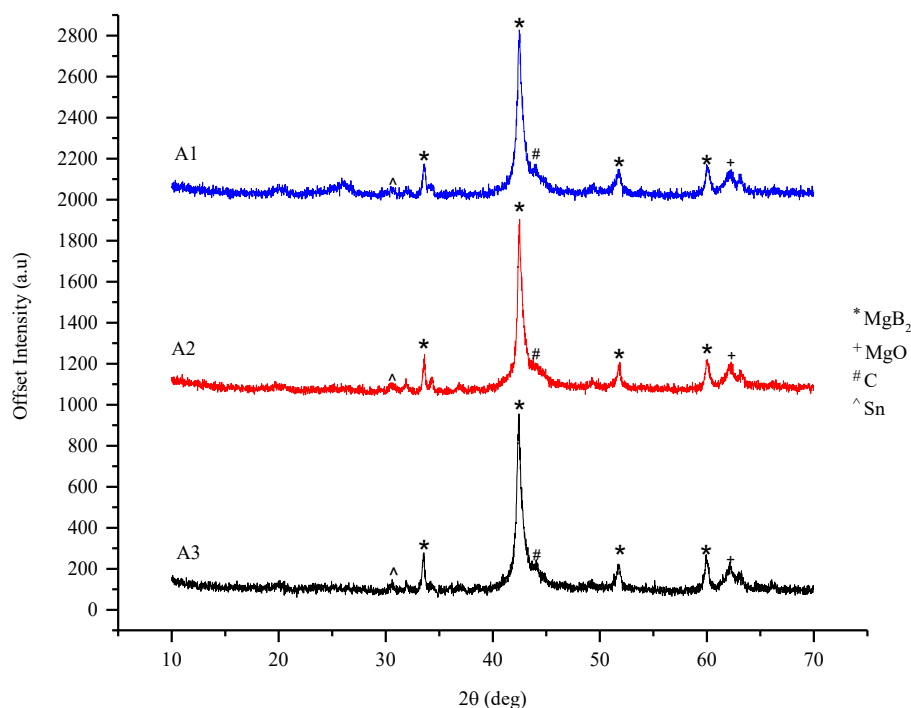


Fig. 1. XRD pattern of the vacuum method

The increase in the amount of multi-walled carbon nanotubes (MWCNTs) dopant, the fractions of MgB_2 , and the impurity phase formed fluctuated (**Table 2**). This was different when observed at the a-constant value, which decreased along with the addition of MWCNTs, but it does not apply to the c-constant. In this case, there is a change in lattice parameters, causing the MgB_2 peak to shift and the number of its intensity to decrease. Nevertheless, the overall ratio of lattice parameters of the MgB_2 phase formed in the vacuum method sample shows a relatively equal value. Based on the qualitative analysis, the carbon phase was not Boron-doped; hence the changes in lattice parameters that occurred in the coded A sample indicated the effect of Sn addition. The most significant volume fraction of impurities in sample A2 and the most significant volume fraction of superconducting phase in sample A1.

Table 2

Mass fraction of the phases in sample A

Sample	The volume fraction of MgB_2 (%)	The volume fraction of impurities (%)	a-const. (Å)	c-const. (Å)	Ratio (c/a)
A1	86.051	13.95	3.0824	3.5297	1.145
A2	81.404	18.59	3.0811	3.5298	1.145
A3	85.212	14.79	3.0793	3.5333	1.147

The various phases are contained in the PIST method sample if to look at **Fig. 2**. Based on the Mg and MgO phases detected, it is assumed that some magnesium synthesized powders have been partially oxidized, and some have not. The reduced intensity of the MgO confirms that the synthesis method with stainless steel SS316 used effectively reduces the possibility of oxidized samples. Also, magnesium powder partially reacts with the tin powder formed in samples B1, B2, and B3. Doping with CNTs has a slightly different effect on phase formation in B1 and B2 and B3

shown at angles around 60–70°. The absence of the Sn phase, as found in the sample codes *A* and *B*, indicates that the tin powder has completely melted.

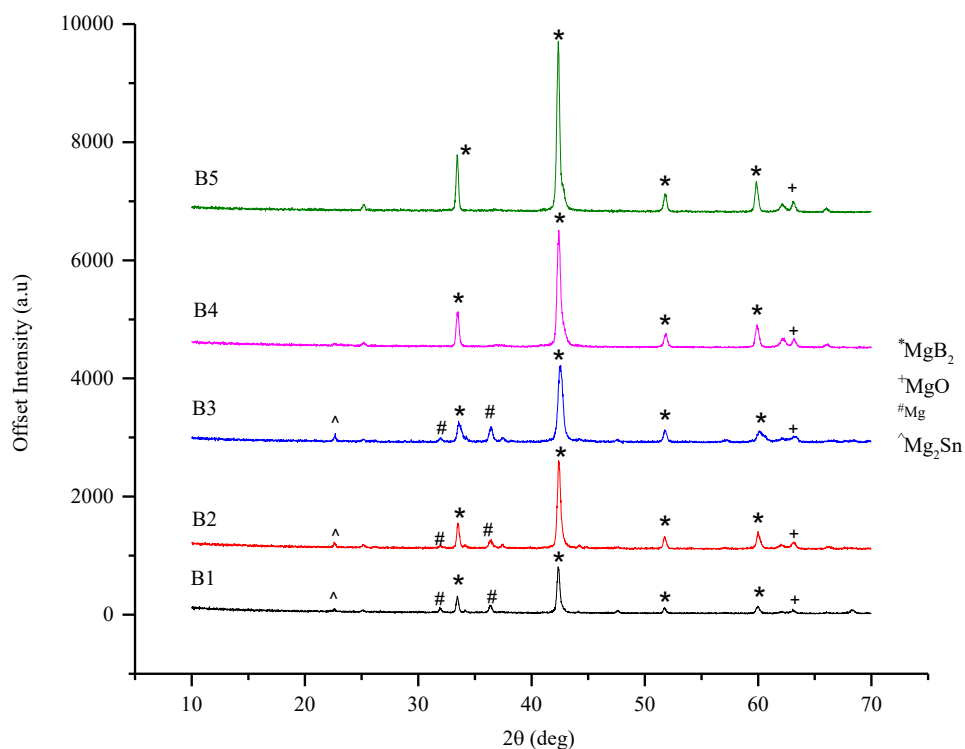


Fig. 2. XRD pattern of the PIST method

Table 3 confirms the dominance of the MgB_2 phase formed in each sample. The impurities fraction formed in the PIST method becomes larger along with the increase in the amount of CNT dopant in *B1*, *B2*, and *B3*, indicating a smaller influence on the a-lattice parameter; however, the c-lattice parameter shows relatively stable results. This is the same as in the vacuum method sample, where there is a change in the a-lattice parameter (but the c-lattice parameter was constant). Meanwhile, the effect of tin powder on *B4* was not significant because the ratio of the lattice parameters was relatively the same as the results obtained with the pure MgB_2 in *B5*. The effect can be observed in the height of intensity in each sample (**Fig. 3**), the higher the addition of CNT will increase the intensity of the XRD data at the dominant peak of MgB_2 .

Table 3

Mass fraction of the phases in sample *B*

Sample	Mass fraction of MgB_2 (%)	Mass fraction of impurities (%)	a-const. (Å)	c-const. (Å)	Ratio (c/a)
<i>B1</i>	76.29	23.71	3.0783	3.5233	1.144
<i>B2</i>	87.25	12.75	3.0776	3.5255	1.145
<i>B3</i>	73.27	26.73	3.0701	3.5259	1.148
<i>B4</i>	95.32	4.67	3.0836	3.5221	1.142
<i>B5</i>	97.22	2.78	3.0858	3.5242	1.142

According to **Fig. 4**, the samples *A1* and *B2* in this characterization represent each synthesis method used. *A1* shows visible CNT particles with clear grain boundaries compared to *B2*, thereby indicating the density between the particles is still low despite the addition of CNT and wetting agent from tin. This condition shows the addition of tin powder to the samples success-

fully melts completely. The results confirm the XRD qualitative analysis, which states there is no Sn phase in sample code B. However, at the magnification of 10.000 X, clumping is still seen in both samples. The distribution of the particles also still looks uneven because there are many CNT grains at some points but few at other issues. Moreover, the microstructure features of mixed MWCNT improved the mechanical properties of the MgB₂ wire, according to a previous study. The diameter and length of the MWCNTs are assumed to be responsible for their alignment, adhesion, and reactivity [21]. The granular structure is still visible. As a result, the addition of Sn to the microstructure increases grain connection [22].

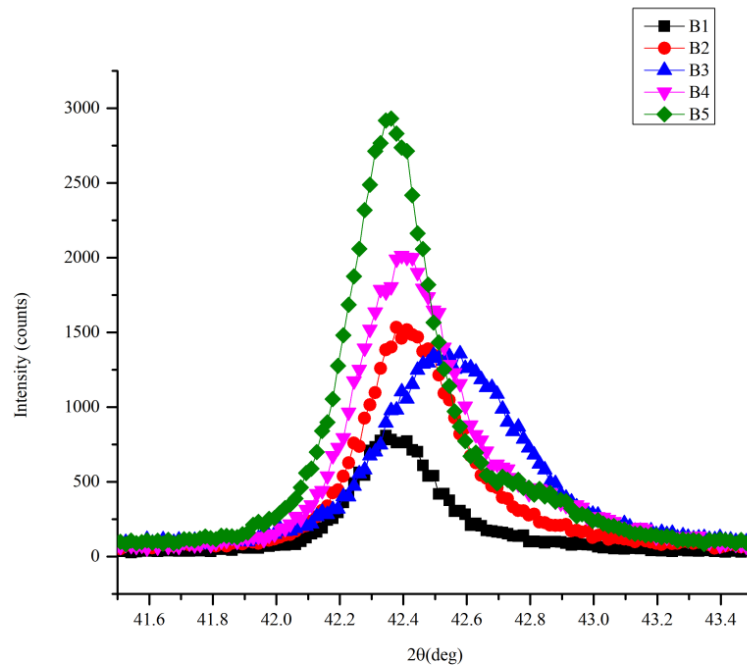


Fig. 3. Peak of the MgB₂ phase at (101) plane

Fig. 5 shows the graph of the resistivity to temperature relationship that indicates the samples in the vacuum method have superconducting characteristics. Each reaction in the presence of cooling treatment causes a decrease in resistivity. By the analysis of phase formation in section 4.1, these three samples have the dominant MgB₂ phase. Sample A1 shows the characteristics of a semiconductor material when 40 K is exceeded, which occurs due to the impurity phases that are still in it, such as MgO, C, and Sn. However, below this temperature, A1 shows superconducting characteristics with a turning point, namely the resistivity decreases dramatically at 35 K. Meanwhile, along with the cooling provided to sample A2, the critical onset temperature (T_{c onset}) is obtained, which is around 80 K, but that of A3 at 40 K. T_{c onset} shows the point where the temperature of the resistivity decreases dramatically. This clarifies that the vacuum method further reduces the superconductivity following the report of previous research [23].

Fig. 6 shows the results of the Cryogenic Magnet test carried out on the PIST method samples, including those in B1, which shows that along with cooling, the trend of stable resistivity decreases at above 40 K. However, once observed more closely at 40 K, the decrease in resistivity is more significant. Based on the XRD testing results, sample B1 has formed a dominant MgB₂ phase. Therefore, the superconductivity phenomenon occurs at a temperature of 40 K. The sample is oxidized only at a low temperature of around 16 K, causing the absence of a transition point. Compared to the previous explanation, the resistivity relationship of sample B2 with temperature shows superconducting characteristics at around 40.5 K. Still, it decreases until the value turns 0 at 40 K. This confirms the XRD results on MgB₂, which is also supported by SEM testing, indicating B2 has a higher density than other samples. This shows that the tin powder has melted entirely, leading to the wetting of other powders for the grain boundaries to become denser and enhance their connectivity.

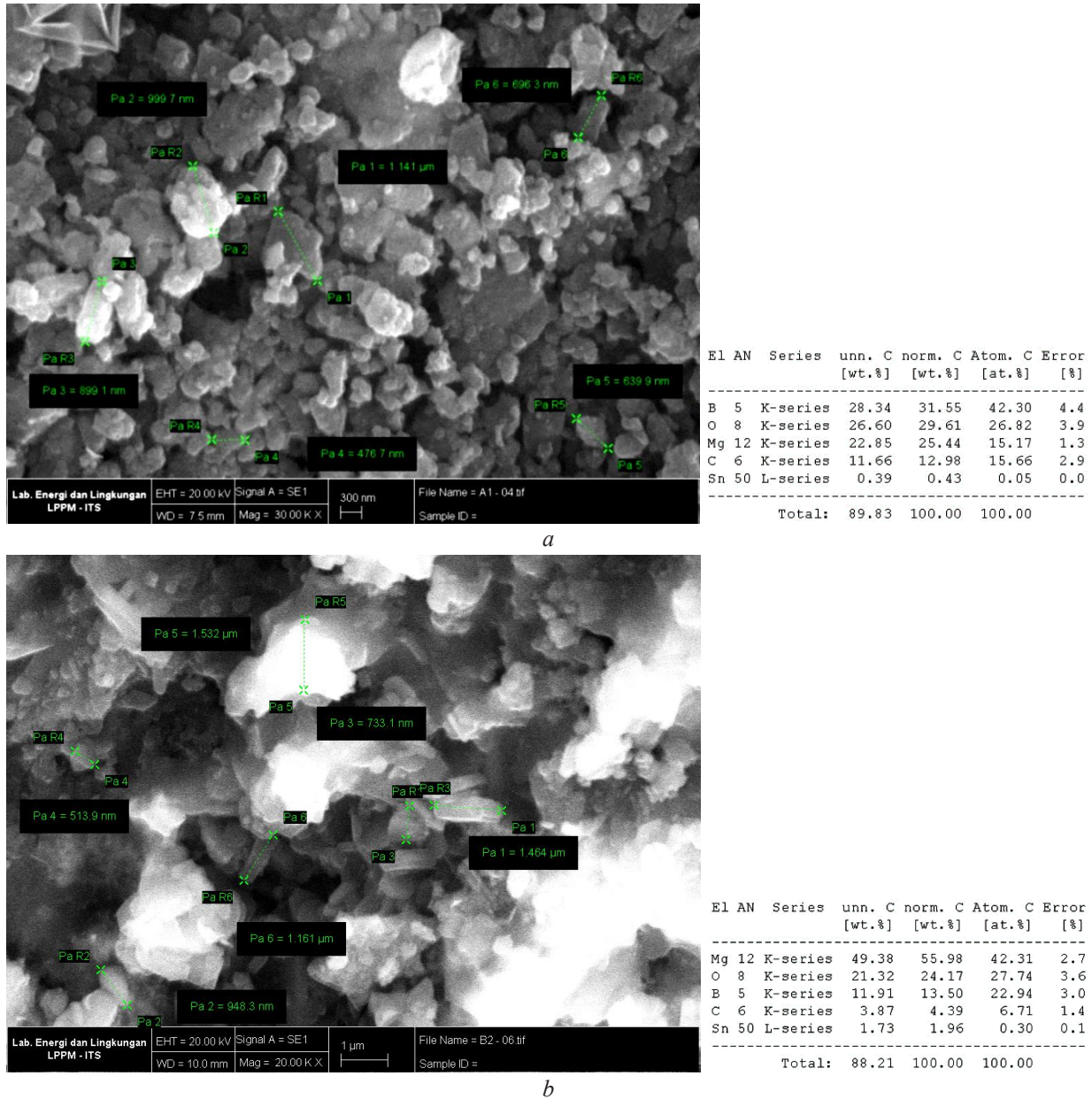


Fig. 4. The microstructure of samples: *a* – A1; *b* – B2

The relationship of resistivity to temperature in sample *B3* shows the T_c onset at a temperature of 40 K, but it does not indicate a zero point. In the temperature range of 38–40 K, only a single phase is formed, meaning that along with the addition of CNT dopant through PIST synthesis, the results are more or less the same as those in the vacuum method sample. Most of the samples show the superconductivity phenomenon around 40 K. As a comparison in this method, MgB_2 samples were synthesized by the addition of tin only, showing a T_c onset at 39 K with T_{c0} at 30 K. These results are supported by XRD testing, which states that MgB_2 is the dominant phase, and MgO is the most minor impurity phase. The absence of the Sn phase indicates that tin powder melts entirely during the sintering process. The melting point of Sn is at a temperature of 231.9 °C, therefore helping in overcoming the influence of the weak link found along the grain boundary. Meanwhile, the results showed the T_c onset of sample *B5* is at around 40 K.

The limitations inherent in this research are the synthesis of materials through the solid-state reaction method and the characterization of samples in the form of bulk to analyze the effect of the addition of CNT, as well as the vacuum sintering method and PIST.

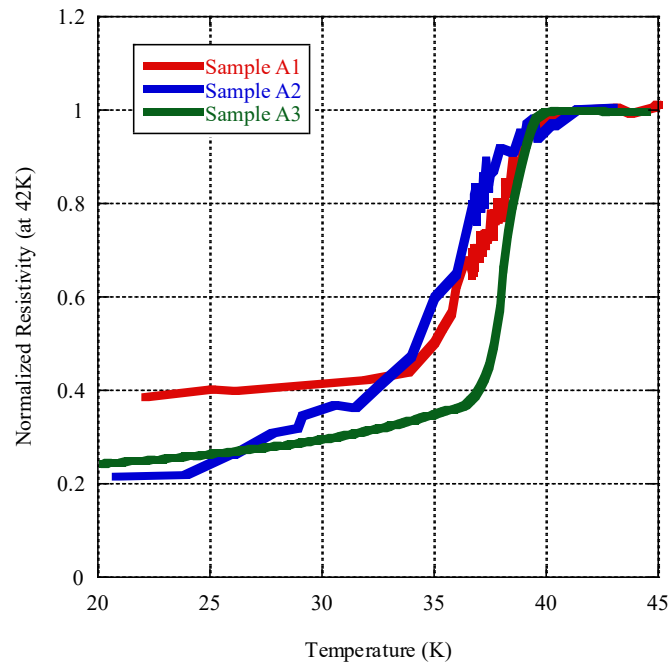


Fig. 5. Normalized Resistivity of vacuum method samples

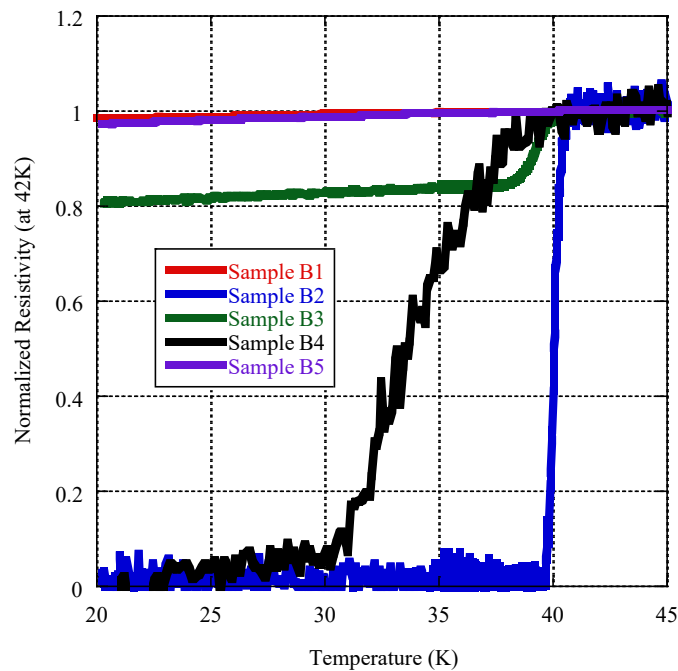


Fig. 6. Normalized Resistivity of PIST method samples

The weakness of this research is that the sample using the vacuum method does not get zero resistivity. The direction of the research needs to be developed to fabricate wire or tape so that it can be applied to MRI coils or superconducting transformers.

4. Conclusions

Based on this study, it can be concluded that the synthesis of MgB_2 superconductors was successfully carried out through the vacuum and PIST methods with a hand milling duration of 3 hours using an agate mortar and sintered temperature of $800\text{ }^\circ\text{C}$ for 2 hours. The effect of variations in CNT addition on the superconductivity of MgB_2 is not too significant where the critical

onset temperature (T_c onset) is at 40 K, except for *A2*, which needs to be tested again to prove the sample results are replicated. According to the diffraction characterization, the dominant phase content in all samples was the MgB_2 with some small impurities. The Scanning Electron Microscope (SEM) showed inhomogeneity in both samples, as only the grain boundaries of *A1* were seen more clearly than *B2*. Meanwhile, Cryogenic Magnet characterization indicated that most synthesized samples had a T_c onset of around 40 K.

Acknowledgment

The authors would like to thank the National Research and Innovation Agency for laboratory equipment facilities and the PLN Institute of Technology for funding research activities with Grant No. 017/1/B04/PU/IT-PLN/2021, as well as researchers and technicians from the Research Center for Metallurgy and Materials-BRIN for their support and assistance in the implementation research and also ELSA BRIN.

References

- [1] Acharya, N., Wolak, M. A., Melbourne, T., Cunnane, D., Karasik, B. S., Xi, X. (2017). As-Grown Versus Ion-Milled MgB_2 Ultrathin Films for THz Sensor Applications. *IEEE Transactions on Applied Superconductivity*, 27 (4), 1–4. doi: <https://doi.org/10.1109/tasc.2016.2645126>
- [2] Morandi, A., Fiorillo, A., Pullano, S., Ribani, P. L. (2017). Development of a Small Cryogen-Free MgB_2 Test Coil for SMES Application. *IEEE Transactions on Applied Superconductivity*, 27(4), 1–4. doi: <https://doi.org/10.1109/tasc.2017.2653202>
- [3] Choi, J. H., Lee, D. G., Jeon, J. H., Lee, E. J., Maeda, M., Choi, S. (2018). Customized MgB_2 Superconducting Wire Toward Practical Applications at Sam Dong in Korea. *Journal of Superconductivity and Novel Magnetism*, 32 (5), 1219–1223. doi: <https://doi.org/10.1007/s10948-018-4814-5>
- [4] Sharma, D., Kumar, J., Vajpayee, A., Kumar, R., Ahluwalia, P. K., Awana, V. P. S. (2011). Comparative Experimental and Density Functional Theory (DFT) Study of the Physical Properties of MgB_2 and AlB_2 . *Journal of Superconductivity and Novel Magnetism*, 24 (6), 1925–1931. doi: <https://doi.org/10.1007/s10948-011-1146-0>
- [5] Xia, J., Li, M., Zhou, Y. (2017). Numerical investigations on the characteristics of thermomagnetic instability in MgB_2 bulks. *Superconductor Science and Technology*, 30 (7), 075004. doi: <https://doi.org/10.1088/1361-6668/aa73b3>
- [6] Kononenko, V. V., Tarenkov, V. Y., Dyachenko, A. I., Varukhin, V. N. (2015). The critical current reaction on hydrostatic pressure of a superconductor-semimetal composite. *Low Temperature Physics*, 41 (3), 199–202. doi: <https://doi.org/10.1063/1.4915909>
- [7] Saito, Y., Murakami, M., Matsumoto, A., Kumakura, H. (2017). Improvement in microstructure and superconducting properties of single-filament powder-in-tube MgB_2 wires by cold working with a swaging machine. *Superconductor Science and Technology*, 30 (6), 065005. doi: <https://doi.org/10.1088/1361-6668/aa6b48>
- [8] Liu, D., Yong, H., Zhou, Y. (2017). A 3-D Numerical Model to Estimate the Critical Current in MgB_2 Wire and Cable with Twisted Structure. *Journal of Superconductivity and Novel Magnetism*, 30 (7), 1757–1765. doi: <https://doi.org/10.1007/s10948-017-4017-5>
- [9] Aldica, G., Burdusel, M., Popa, S., Enculescu, M., Pasuk, I., Badica, P. (2015). The influence of heating rate on superconducting characteristics of MgB_2 obtained by spark plasma sintering technique. *Physica C: Superconductivity and Its Applications*, 519, 184–189. doi: <https://doi.org/10.1016/j.physc.2015.10.004>
- [10] Xia, Q., Yi, J., Peng, Y., Luo, S., Li, L. (2008). Microwave direct synthesis of MgB_2 superconductor. *Materials Letters*, 62 (24), 4006–4008. doi: <https://doi.org/10.1016/j.matlet.2008.05.043>
- [11] Kurama, H., Erkuş, S. (2019). The effect of milling conditions on the magnetic and topological properties of MgB_2 synthesized by high-energy ball mill and sintered at low temperature. *Journal of the Australian Ceramic Society*, 56 (2), 559–566. doi: <https://doi.org/10.1007/s41779-019-00365-z>
- [12] Bhagurkar, A. G., Yamamoto, A., Dennis, A. R., Durrell, J. H., Aljohani, T. A., Nadendla, H. B., Cardwell, D. A. (2017). Microstructural evolution in infiltration-growth processed MgB_2 bulk superconductors. *Journal of the American Ceramic Society*, 100 (6), 2451–2460. doi: <https://doi.org/10.1111/jace.14792>
- [13] Erdem, O., Yanmaz, E. (2015). Effect of Er doping on the superconducting properties of porous MgB_2 . *Bulletin of Materials Science*, 38 (1), 89–93. doi: <https://doi.org/10.1007/s12034-014-0810-y>
- [14] Grivel, J.-C., Pitillas, A., Namazkar, S., Alexiou, A., Holte, O. J. (2016). Preparation and characterization of MgB_2 with Pd, Pt and Re doping. *Physica C: Superconductivity and Its Applications*, 520, 37–41. doi: <https://doi.org/10.1016/j.physc.2015.11.001>
- [15] Shahabuddin Shah, M., Shahabuddin, M., Parakkandy, J. M., Qaid, S., Alzayed, N. S. (2015). Enhanced critical current density in undoped MgB_2 prepared by in situ/ex situ combination technique. *Solid State Communications*, 218, 31–34. doi: <https://doi.org/10.1016/j.ssc.2015.06.004>

- [16] Xiong, J., Cai, Q., Ma, Z., Yu, L., Liu, Y. (2014). Enhancement of Critical Current Density in MgB₂ Bulk with CNT-coated Al Addition. *Journal of Superconductivity and Novel Magnetism*, 27 (7), 1659–1664. doi: <https://doi.org/10.1007/s10948-014-2513-4>
- [17] Cai, Q., Liu, Y., Ma, Z., Yu, L. (2013). Comparison of carbon-doped MgB₂ bulks fabricated from pre-synthesized Mg/CNT and Mg/amorphous carbon composites. *Applied Physics A*, 114 (3), 919–924. doi: <https://doi.org/10.1007/s00339-013-7764-6>
- [18] Imaduddin, A., Samsulludin, Wicaksono, M. R., Saefuloh, I., Herbirowo, S., Yudanto, S. D. et. al. (2019). The Doping Effects of SiC and Carbon Nanotubes on the Manufacture of Superconducting Monofilament MgB₂ Wires. *Materials Science Forum*, 966, 249–256. doi: <https://doi.org/10.4028/www.scientific.net/msf.966.249>
- [19] Shahabuddin, M., Madhar, N. A., Alzayed, N. S., Asif, M. (2019). Uniform Dispersion and Exfoliation of Multi-Walled Carbon Nanotubes in CNT-MgB₂ Superconductor Composites Using Surfactants. *Materials*, 12 (18), 3044. doi: <https://doi.org/10.3390/ma12183044>
- [20] Ahmad, I., Hansdah, J. S., Sarangi, S. N., Sarun, P. M. (2020). Enhanced magnetic field dependent critical current density of MWCNT doped magnesium diboride superconductor. *Journal of Alloys and Compounds*, 834, 155033. doi: <https://doi.org/10.1016/j.jallcom.2020.155033>
- [21] Patel, D., Maeda, M., Choi, S., Kim, S. J., Shahabuddin, M., Parakandy, J. M. et. al. (2014). Multiwalled carbon nanotube-derived superior electrical, mechanical and thermal properties in MgB₂ wires. *Scripta Materialia*, 88, 13–16. doi: <https://doi.org/10.1016/j.scriptamat.2014.06.010>
- [22] Fujii, H., Kitaguchi, H. (2020). Reduced sintering temperature in ex situ processed MgB₂ tapes using filling powders with Sn addition. *Physica C: Superconductivity and Its Applications*, 576, 1353704. doi: <https://doi.org/10.1016/j.physc.2020.1353704>
- [23] Ozturk, O., Asikuzun, E., Kaya, S., Erdem, M., Safran, S., Kilic, A., Terzioglu, C. (2015). Ac Susceptibility Measurements and Mechanical Performance of Bulk MgB₂. *Journal of Superconductivity and Novel Magnetism*, 28 (7), 1943–1952. doi: <https://doi.org/10.1007/s10948-015-3003-z>

Received date 14.10.2021

Accepted date 02.05.2022

Published date 31.05.2022

© The Author(s) 2022

This is an open access article
under the Creative Commons CC BY license

How to cite: Hendrik, H., Nur Farhanudin, M., Darsono, N., Herbirowo, S., Darminto, D., Pramono, A. W., Imaduddin, A. (2022). Synthesis and characterization of MgB₂ superconductors with carbon nanotubes (CNTs) and tin (Sn) addition. *EUREKA: Physics and Engineering*, 3, 91–100. doi: <https://doi.org/10.21303/2461-4262.2022.002419>